Journal of Power Sources 196 (2011) 6978–6981

Contents lists available at ScienceDirect

Journal of Power Sources

journal homepage: www.elsevier.com/locate/jpowsour

Short Communication

# A $^{57}$Fe Mössbauer spectroscopy study of cobalt ferrite conversion electrodes for Li-ion batteries

Candela Vidal-Abarca, Pedro Lavela, José L. Tirado*

*Laboratorio de Química Inorgánica, Universidad de Córdoba, Edificio Maire Curie, Planta 1, Campus de Rabanales, 14071 Córdoba, Spain*

ARTICLE INFO

*Article history:*
Received 22 July 2010
Received in revised form 19 October 2010
Accepted 29 October 2010
Available online 9 November 2010

*Keywords:*
Lithium-ion batteries
Cobalt ferrite
Conversion reaction
Mössbauer spectroscopy

ABSTRACT

The reverse micelles method has been employed to obtain cobalt ferrite samples. The effect of the type of surfactant and volumetric proportion of the aqueous and organic phases on the electrochemical behavior has been evaluated. The sample prepared using Span 80 as a surfactant and equivalent volumes of the aqueous and organic phases showed the highest capacity values and rate capabilities. It has been correlated to the better stability of the faradaic conversion process upon cycling for this sample. Based on the $^{57}$Fe Mössbauer spectra of discharged electrodes, this result has been associated to the preservation of reduced iron atoms into the core of the particles. The metallic atoms are ready to be oxidized, thus sustaining the reversible electrochemical reaction in further cycles.



## 1. Introduction

Transition metal oxides and oxysalts display interesting conversion reactions in lithium cells [1]. The effective reversible reduction of metal atoms from the initial oxidation state to the metallic state involves the transfer of several electrons. This is the main advantage of these electrode materials. Reversible capacities close to twice the theoretical capacity of graphite are commonly observed, which gives these materials a potential applicability in lithium-ion batteries [2]. The electrochemical reversibility of these reactions has been ascribed to the nanometric size of the particles of the products (M and $Li_2O$) [3]. It ensures an extremely large interface which facilitates the slow oxide ion migration between the metal atoms. Nevertheless, the significant polarization between charge and discharge branches and high irreversible capacities in the first cycle jeopardizes their practical use.

Recently, it has been shown the interest of ternary oxides as $Co_{3-x}Fe_xO_4$ ($x$ = 0, 1, 2) or the $Mn_xCo_{3-x}O_4$ series ($x$ = 1, 1.5, 2, 3) to tune the anode working voltage [4,5]. The presence of two different transition metals leads to a unique reduction plateau whose potential depends on the stoichiometry and the metal present in the composition. Also, the morphology of both primary particles and their agglomerates has a notorious influence on the electrochemical performance [6,7]. Therefore, the analysis of new method of synthesis affecting to the size and shape of the particles may lead to new materials with optimized electrochemical properties [8,9]. In this way, the reverse micelles method is an alternative preparation route based on the use of organic anionic surfactants that stabilize reverse (water-in-oil) micelles [10,11]. The transition metal solution reacts within the small aqueous droplets to yield a solid precursor.

In order to develop new methods to limit the main drawbacks, a first step is always a good understanding of the reaction mechanisms. For this purpose, $^{57}$Fe Mössbauer spectroscopy (MS) has proven to be a relevant tool in the study of iron containing oxides [12,13]. In this communication we discuss the mechanism of reduction–reoxidation of $CoFe_2O_4$ in lithium test cells, using MS.

## 2. Experimental

The precursor formation undergoes by the coalescence of two different reverse micelles containing aqueous solutions of metal chlorides as a metal source and 8 M NaOH solution as precipitating reagent. The reverse micelles were stabilized by stirring the aqueous solution in an organic phase in the presence of a surfactant. The organic phase selected for this procedure was hexane. The aqueous to organic volume ratio was allowed to vary from 1:1 to 1:2. Span 80 and Tween 85 surfactants were used. The precursors were eventually annealed in air at 800 °C for 15 h. Samples will be named as CoFeXA:B (X:S or T for the surfactant; A:B for the aqueous:organic phase ratio). Thus, samples will be named as CoFeS1:1, CoFeS1:2 and CoFeT1:1.

X-ray diffraction (XRD) patterns were recorded in a Siemens D5000 diffractometer, with a Cu Kα radiation and a graphite

* Corresponding author. Tel.: +34 957218637; fax: +34 957218621.
*E-mail address:* iq1ticoj@uco.es (J.L. Tirado).

0378-7753/$ – see front matter © 2010 Elsevier B.V. All rights reserved.
doi:10.1016/j.jpowsour.2010.10.101

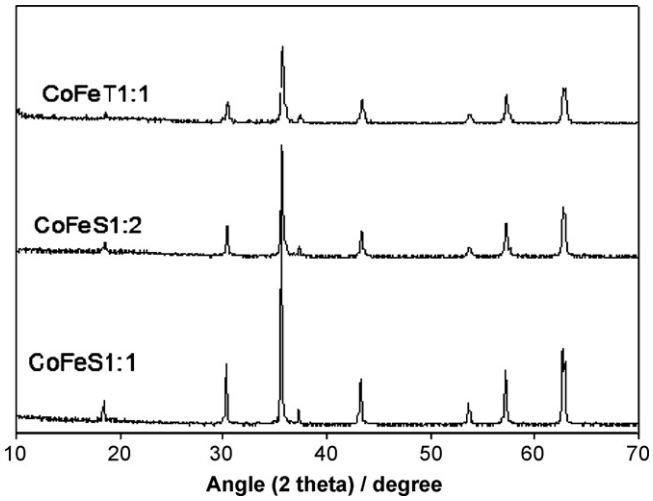


**Fig. 1.** XRD patterns of the annealed samples.

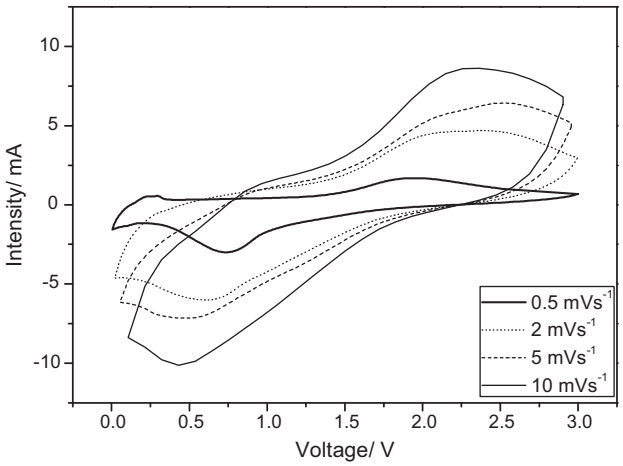


**Fig. 3.** SPES results at different rates for sample CoFeS1:1.

monochromator. SEM images were obtained with a JEOL-SM6300 microscope. An EG&G constant acceleration spectrometer and a $^{57}$Co (Rh matrix) gamma radiation source were used for recording $^{57}$Fe Mössbauer spectra in transmission mode at room temperature. The magnetic sextet recorded from a high purity iron foil was used to calibrate the velocity scale. Experimental data were fitted to Lorentzian lines using a least square based method [14].

Battery tests were carried out using two-electrodes Swagelok type cells. Counter electrodes were 9 mm discs of lithium metal and the working electrode consisted of a mixture of 75% of active material and 10% of graphite, 10% of carbon black and 5% of PVDF binder was coated on a cooper foil of the same diameter. A 1 M $LiPF_6$ (EC:DEC = 1:1) electrolyte solution was supported in Whatman glass fiber discs. Galvanostatic tests were carried out on an Arbin galvanostat multichannel system. The imposed kinetic rate was set at 1*C* for battery testing and *C*/2 for the discharged electrodes used in the Mössbauer spectroscopy. Step potential electrochemical spectroscopy (SPES) was monitored on a MacPile System.

## 3. Results and discussion

The XRD patterns of the annealed products were characterized by narrow and intense reflections that can be indexed in the Fd3m space group corresponding to $CoFe_2O_4$ (JCPDS 03-0864) (Fig. 1). The presence of impurities was discarded. The reflections of the CoFeS1:1 sample are less broadened that is related to the higher crystallinity of this sample.

The analysis of the SEM images showed the occurrence of large agglomerates of primary particles (Fig. 2). It evidenced a close similarity between the oxides prepared using Span 80 as a surfactant irrespective of the volume ratio of aqueous and organic phases. They were constituted by submicron particles. Contrarily, the use of Tween 85 as a surfactant involved the presence of large primary particles with a micrometric size. This different morphology would influence undoubtedly on the electrochemical behavior, since lithium reacts with the electrode material migrating from the surface to the core particle.

The electrochemical lithium driven conversion reaction can be decomposed in two different processes. First, a faradaic process involves the complete reduction of the metal atoms. This effect is identified by an extended plateau which voltage is located slightly higher than 1 V for the cobalt ferrite. Then a pseudo-capacitive process appears as a sloping voltage feature until the end of discharge. The relative contribution of both processes depends on several factors as the sweep rate. Fig. 3 shows the SPES results obtained at different rates, *v*, for sample CoFeS1:1, which were used to calculate the relative contributions using the method developed by Dunn and coworkers [15,16]. A linear relationship was found between the intensity measured at different voltages using Eq. (1).

$$\frac{i(V)}{v^{1/2}} = k_1 v^{1/2} + k_2 \quad (1)$$

where constants $k_1$ and $k_2$ are related to current contributions from surface capacitive and diffusion-controlled faradaic effects, respectively. As can be seen in Table 1, the contribution of the faradaic reaction increases with the sweep rate from 2 mV $s^{-1}$ what evidences the importance of this process to favor high rate capabilities. However, for slow rates of 0.5 mV $s^{-1}$ this tendency is reverted probably due to the higher contribution of other electrochemical

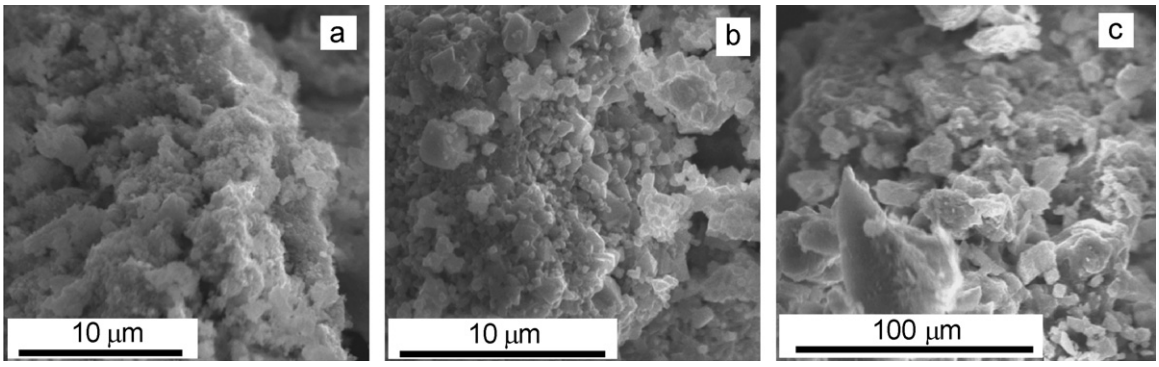


**Fig. 2.** SEM images of $CoFe_2O_4$ samples with (a) CoFeS1:1; (b) CoFeS1:2 and (c) CoFeT1:1.

**Table 1**
Relative contributions of faradaic and capacitive processes to the total discharge capacity at different sweep rates for CoFeS1:1.

| Sweep rate ($mV\,s^{-1}$) | Capacitive (%) | Faradaic (%) |
|---|---|---|
| 0.5 | 17.85 | 82.15 |
| 2 | 36.46 | 63.54 |
| 5 | 16.95 | 83.05 |
| 10 | 14.24 | 85.76 |

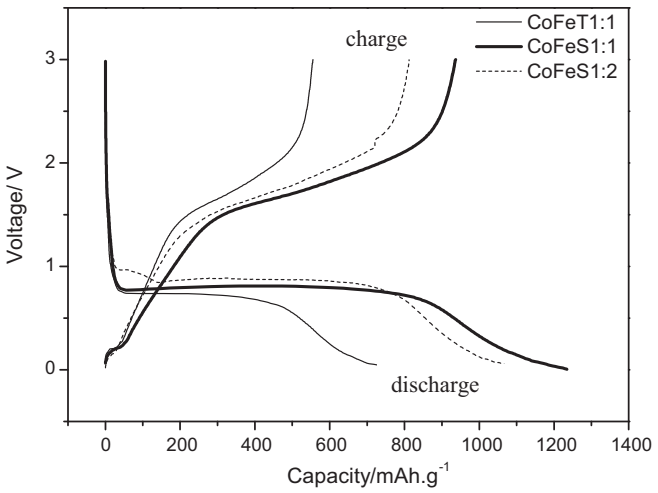


**Fig. 4.** Voltage profiles with discharge/charge capacities for the studied samples.

processes, such as reactions with the electrolyte which are kinetically hindered at higher rates.

For electrochemical characterizations, voltage profiles with discharge/charge capacities and first cycle efficiency were obtained. The profiles have been included in new Fig. 4. The efficiencies were 75.8, 74.4 and 73.4% for CoFeS1:1, CoFeS1:2, and CoFeT1:1, respectively. The extended galvanostatic cycling reveals quite different behaviors for the obtained samples despite the equivalent composition (Fig. 5). It highlights the importance of morphological and crystallinity differences on the performance of these electrode materials subjected to conversion reactions. Thus, CoFeS1:1 showed the highest capacity retention reaching capacity values as high as 614 mAh $g^{-1}$ after 50 cycles.

In order to understand their different performances the differential capacity plots were displayed in Fig. 6. The 2nd, 10th, 20th and 40th cycles were plotted to evidence the general behavior upon cycling. The bands are correlated to the galvanostatic quasi-plateaus defining the faradaic process. The positive values correspond to the charging curves. The strongly broadened bands are ascribed to the transition metal oxidation reactions. Unfortunately, their enhanced broadening avoids description of the different behaviors among samples. Contrarily, the anodic process is characterized by narrow signals which evolution upon cycling allows discerning some differences among the studied samples. As a general feature, we observe a progressive shifting of the signals to lower voltages. This effect could be related to an increase in electrode polarization. This effect could be attributed to a decrease in the electronic conductivity due to particle isolation. The capacity fading of CoFeS1:2 and CoFeT1:1 samples can be correlated to the decrease in intensity and enhanced broadening observed in these faradaic signals upon cycling. It undoubtedly reflects the lack of stability of the electrochemical reaction after a large number of cycles.

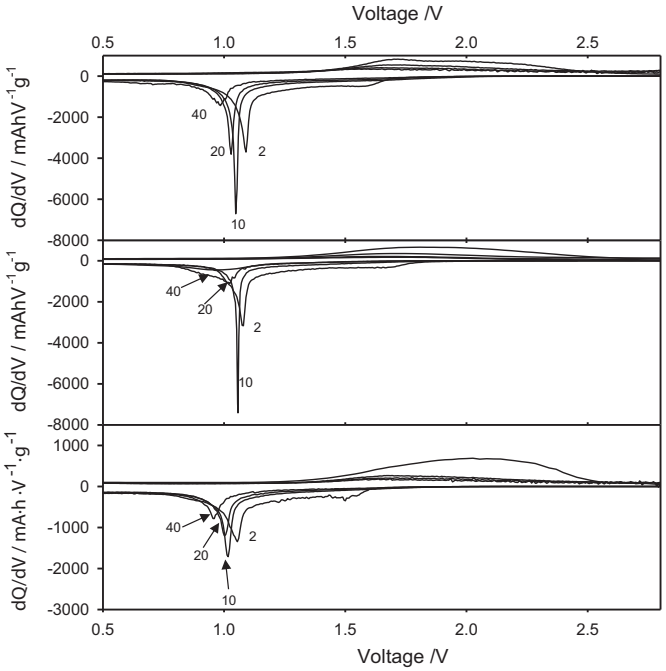


**Fig. 6.** Differential capacity plots of (a) CoFeS1:1; (b) CoFeS1:2; and (c) CoFeT1:1.

The better stability of the faradaic process can be also evidenced observing the rate capability. Thus, the sample CoFeS1:1 is able to

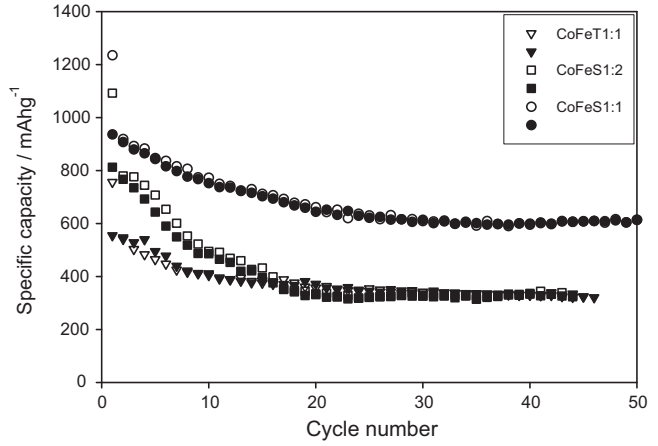


**Fig. 5.** Galvanostatic cycling of the studied samples (open circles: discharge and full symbol: charge).

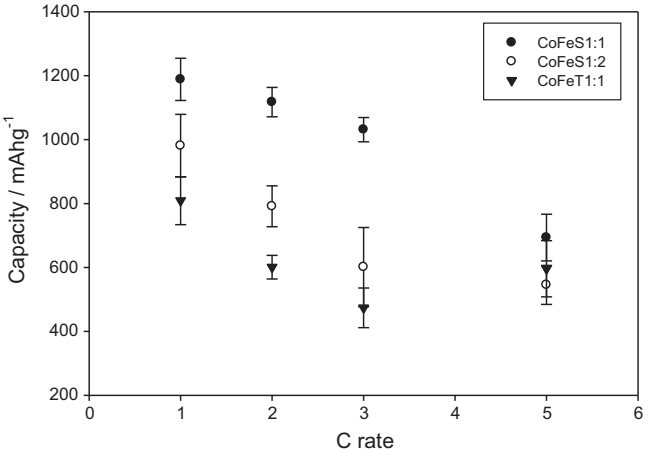


**Fig. 7.** Plot of specific capacity values recorded for the first discharge at several kinetic rates.

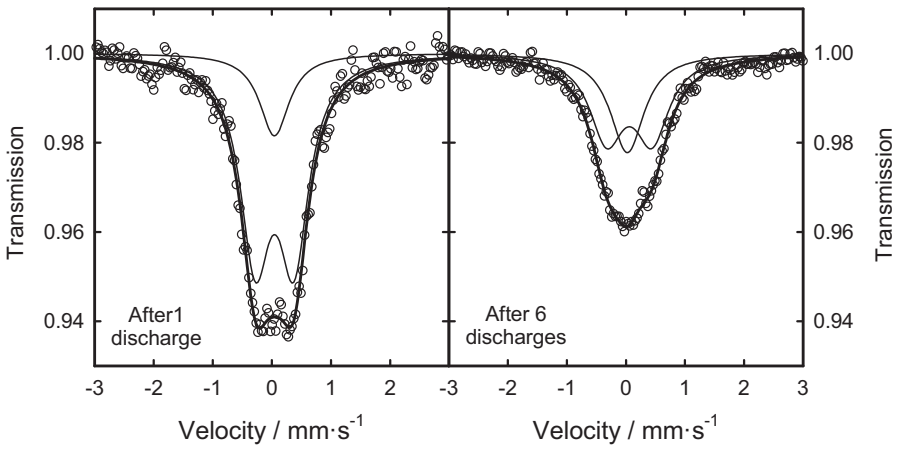


**Fig. 8.** $^{57}$Fe Mössbauer spectra of CoFeS1:1 electrodes recorded after (a) one and (b) six discharges.

sustain high capacity values when subjected to high *C* rates (Fig. 7). Nevertheless, an enhanced decrease in capacity was recorded for this sample when discharged at 5*C*.

The $^{57}$Fe Mössbauer spectra of CoFeS1:1 discharged electrodes can be decomposed into a doublet and a singlet revealing the superparamagnetic character of the metallic Fe obtained upon the electrochemical reduction (Fig. 8). The isomer shift values ranging between 0.0 and 0.07 mm s$^{-1}$ confirm the effective reduction of the transition metal. The singlet is commonly assigned to Fe atoms located at the core of the particles, while the doublet is attributed to those placed on the surface. Moreover, the isomer shift value of the latter doublet is usually higher than that of core iron atoms. It has been attributed to the contact of surface iron atoms with the electrolyte favoring undesirable oxidation side reactions with the electrolyte which increases their average oxidation state and also enhances the irreversibility of the electrochemical reaction. Otherwise, core iron atoms are preserved from these side reactions and contribute positively to the reversibility of the redox reaction. In fact, a decrease in the relative contribution of the singlet upon cycling has been correlated to the capacity fading in related electrode materials [7]. Therefore, the high contribution of core iron atoms to the overall spectrum after six cycles in CoFeS1:1 may explain its high capacity retention after a large number of cycles.

## 4. Conclusions

The reverse micelles method is a suitable route to prepare anode materials undergoing electrochemical conversion reactions. The appropriated selection of the synthesis conditions, namely type of surfactant and aqueous/organic phase volume ratio, leads to electrode materials with optimized electrochemical performance. $CoFe_2O_4$ sample prepared using Span 80 as a surfactant and a ratio of 1:1 showed the highest capacity values (614 mAh g$^{-1}$) after a large number of cycles. The contribution of the faradaic process to the electrochemical performance during the galvanostatic cycling has demonstrated to be essential. This effect has been correlated to the preservation of metallic iron atoms into the core of the particles in the discharged electrodes. These atoms are preserved from irreversible reactions with the electrolyte and hence they promote the high reversibility and rate capability of CoFeS1:1 sample.

## Acknowledgments

We appreciate the financial support from the MICINN (Contract MAT2008-0558) and Government of Andalusia (Project FQM1447, group FQM288). CV is grateful to MICINN for a FPI grant. We also want to thank the Central Support Service for Research at the University of Cordoba.

## References

[1] M.J. Aragón, P. Lavela, B. León, C. Pérez-Vicente, J.L. Tirado, C. Vidal-Abarca, J. Solid State Electrochem. 14 (2010) 1749.
[2] P. Lavela, J.L. Tirado, J. Power Sources 172 (2007) 379.
[3] P. Poizot, P.S. Laruelle, S. Grugeon, L. Dupont, J.M. Tarascon, Nature 407 (2000) 496.
[4] P. Lavela, G.F. Ortiz, J.L. Tirado, E. Zhecheva, R. Stoyanova, Sv. Ivanova, J. Phys. Chem. C 111 (38) (2007) 14238.
[5] P. Lavela, J.L. Tirado, C. Vidal-Abarca, Electrochim. Acta 52 (2007) 7986.
[6] Q. Fan, M.S. Whittingham, Electrochem. Solid State Lett. 10 (2007) A48.
[7] F. Gillot, S. Boyanov, L. Dupont, M.L. Doublet, M. Morcrette, L. Monconduit, J.M. Tarascon, Chem. Mater. 17 (2005) 6327.
[8] J. Akl, T. Ghaddar, A. Ghanem, H. El-Rassy, J. Mol. Catal. A: Chem. 312 (2009).
[9] S. Grugeon, S. Laruelle, R. Herrera-Urbina, L. Dupont, P. Poizot, J.M. Tarascon, J. Electrochem. Soc. 148 (2001) A285.
[10] G.X. Wang, Y. Chen, L. Yang, J. Yao, S. Needham, H.K. Liu, J.H. Ahn, J. Power Sources 146 (2005) 487.
[11] C. Vidal-Abarca, P. Lavela, J.L. Tirado, Electrochem. Solid State Lett. 11 (2008) A198.
[12] P. Lavela, J.L. Tirado, M. Womes, J.C. Jumas, J. Electrochem. Soc. 156 (2009) A589.
[13] P. Lavela, J.L. Tirado, M. Womes, J.C. Jumas, J. Phys. Chem. C 113 (2009) 20081.
[14] W. Kündig, Nucl. Instr. Methods 75 (1969) 336.
[15] J. Wang, J. Polleux, J. Lim, B. Dunn, J. Phys. Chem. C 111 (2007) 14925.
[16] T. Brezesinski, J. Wang, J. Polleux, B. Dunn, S.H. Tolbert, J. Am. Chem. Soc. 131 (2009) 1802.